ARTICLE

Preparation of Covalently Functionalized Graphene Using Residual Oxygen-Containing Functional Groups

Min-Chien Hsiao,[†] Shu-Hang Liao,[†] Ming-Yu Yen,[†] Po-I Liu,[†] Nen-Wen Pu,[‡] Chung-An Wang,[‡] and Chen-Chi M. Ma*[,†]

Department of Chemical Engineering, National Tsing Hua University, Hsinchu 30013, Taiwan and Department of Applied Chemistry and Materials Science, Chung Cheng Institute of Technology, National Defense University, Taoyuan 33448, Taiwan

ABSTRACT When fabricated by thermal exfoliation, graphene can be covalently functionalized more easily by applying a direct ring-opening reaction between the residual epoxide functional groups on the graphene and the amine-bearing molecules. Investigation by X-ray photoelectron spectroscopy (XPS), Raman spectroscopy, and transmission electron microscopy (TEM) all confirm that these molecules were covalently grafted to the surface of graphene. The resulting dispersion in an organic solvent demonstrated a long-term homogeneous stability of the products. Furthermore, comparison with traditional free radical functionalization shows the extent of the defects characterized by TEM and Raman spectroscopy and reveals that direct functionalization enables graphene to be covalently functionalized on the surface without causing any further damage to the surface structure. Thermogravmetric analysis (TGA) shows that the nondestroyed graphene structure provides greater thermal stability not only for the grafted molecules but also, more importantly, for the graphene itself, compared to the free-radical grafting method.

KEYWORDS: Covalent Functionalization • Graphene • Thermal Reduction • Residual Oxygen-Containing Functional Groups • Thermal stability

INTRODUCTION

Graphene is a new material used in the development of novel nanomaterials in various applications and consists of a single layer of carbon atoms densely packed in a two-dimensional honeycomb lattice (1). Its defining features are its unusual electronic character (with carrier mobilities of up to 200 000 $cm^2 V^{-1} s^{-1}$) (2, 3), high thermal conductivity (~4840−5300 $W m^{-1} K^{-1}$) (4), good mechanical properties, high elasticity (5), and high specific surface area (~2600 $m^2 g^{-1}$) (6). A number of researchers have developed a range of approaches to synthesize graphene, including micromechanical cleavage (7, 8), liquid-phase exfoliation of graphite (9, 10), epitaxial growth (11, 12), and reduction from graphite oxide (GO), the precursor of graphene, by chemical (13−16) or thermal exfoliation (17−19). Among these methods, the oxidation of graphite to GO and subsequent thermal reduction is the best bulk production method for many applications, especially for polymer composites (17, 19−21). Although graphene is functionalized when reduced from GO (20−22), the residual oxidized functional groups are not sufficient to sustain the high surface area necessary for long-term stable dispersion in solvents. Therefore, for many applications, it is necessary to modify the surface of graphene in order to dissolve it in the required solvents, or to increase the interfacial interaction between the matrix and graphene. In order to undertake a comprehensive survey of graphene functionalization, it must be understood that there are three main methods of functionalization: (i) noncovalent attachment of large/small aromatic-containing molecules through $\pi-\pi$ stacking (23−26); (ii) grafting molecules on the basal plane of graphene (13, 27−29); (iii) chemical reactions between the functional groups on GO and other molecules, together with subsequent or simultaneous chemical reduction (30−33). The advantage of using noncovalent attachment is that it functionalizes the graphene surface without risking significant damage to it. However, the forces of physical interaction might be weak, making the load transfer efficiency of the reinforcement of the composites quite low. Even when chemical grafting creates strong bonding between graphene and the attached molecules, it produces additional defects on the graphene surface and, hence, weakens the structure of the graphene. In order to overcome these problems, method iii above may offer a better way to functionalize graphene through chemical bonding. However, this method is not suitable for functionalizing graphene produced by thermal exfoliation (>550 °C (34)).

Recently, Boukhvalov and Katsnelson (35) and Gao et al. (36) used density functional theory to investigate the structure of graphene after deoxygenation. Interestingly, both groups of researchers confirmed that it was impossible to remove completely the oxygen-containing functional groups from the graphene surface using chemical or thermal reduc-

* Corresponding author. Tel.: 886-35713058. Fax: 886-35715408. E-mail: ccma@che.nthu.edu.tw.
Received for review July 8, 2010 and accepted September 29, 2010
[†] National Tsing Hua University.
[‡] National Defense University.
DOI: 10.1021/am100597d

Published on Web 10/15/2010

Scheme 1. The Preparation of F-Graphene/MA-POA2000 and D-Graphene/MA-POA2000

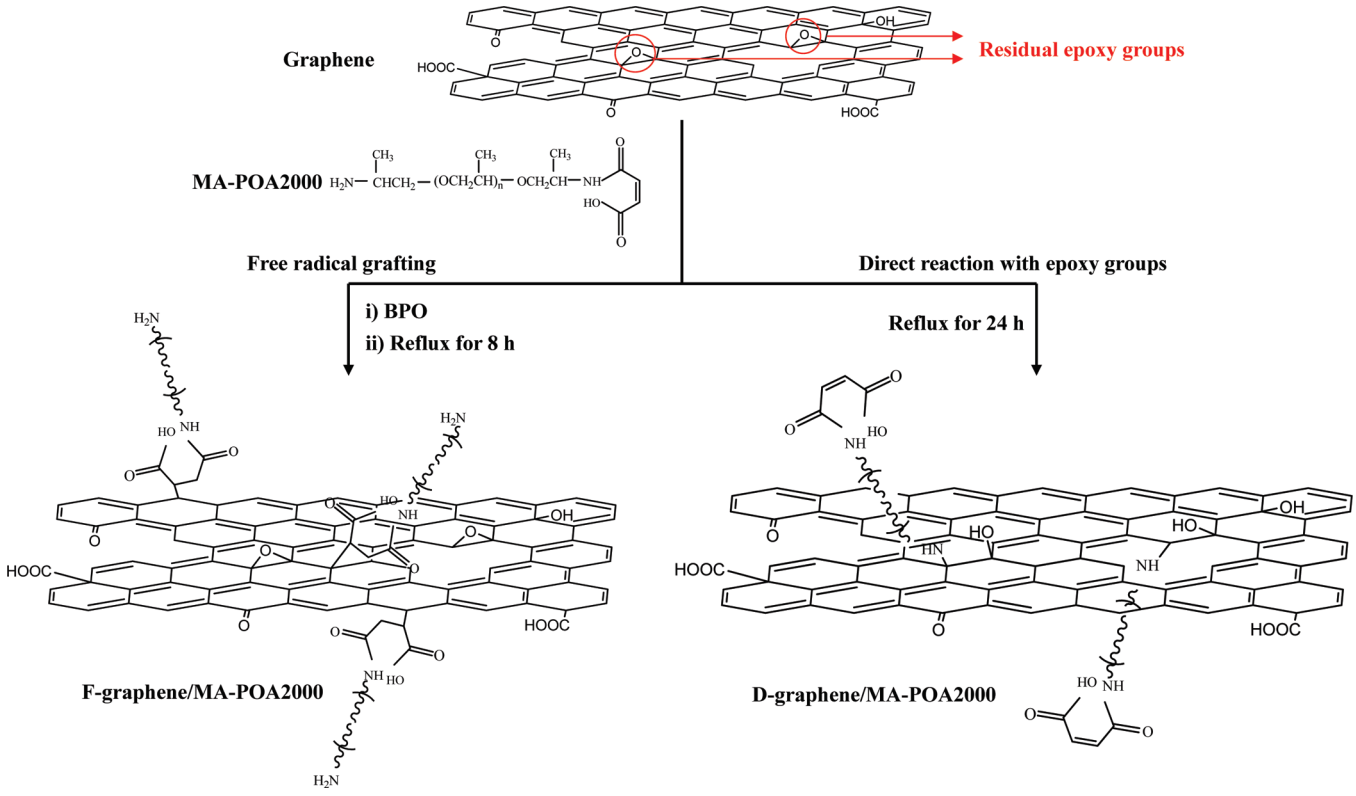

tion, or even a combination of the two. Experimentally, to the best of our knowledge, all of the results of characterization of graphene fabricated from GO show the existence of the residual oxygen-containing functional groups on the graphene. From the collection of available theoretical and experimental results, we believe that finding the most efficient way to deal with these unremovable residual functional groups would also be a useful topic for study. We suggest that there are three advantages to the use of these residual oxygen-containing functional groups for covalent functionalization: (i) The restored graphene structures with a high sp^2 fraction will not be harmed during functionalization. (ii) Although using the abundant oxygen-containing functional groups of GO to react with chemical molecules, followed by subsequent chemical reduction, can be used to prepare functionalized graphene, the degree of reduction may be somewhat limited. This is because the oxygen-containing functional groups are not just the reactive sites,

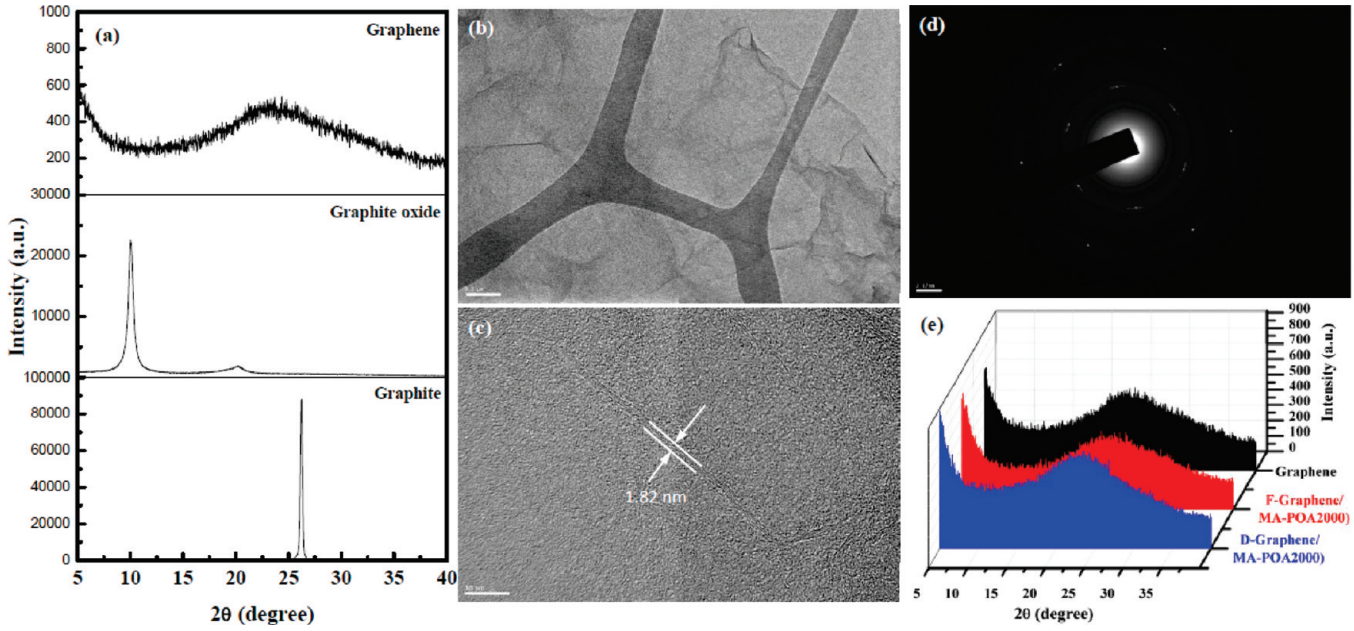

FIGURE 1. (a) XRD spectra of pristine graphite, graphite oxide, and graphene; TEM observation of graphene using (b) low magnification and (c) high magnification; (d) the SAED pattern; (e) XRD spectra of graphene, F-graphene/MA-POA2000, and D-graphene/MA-POA2000.

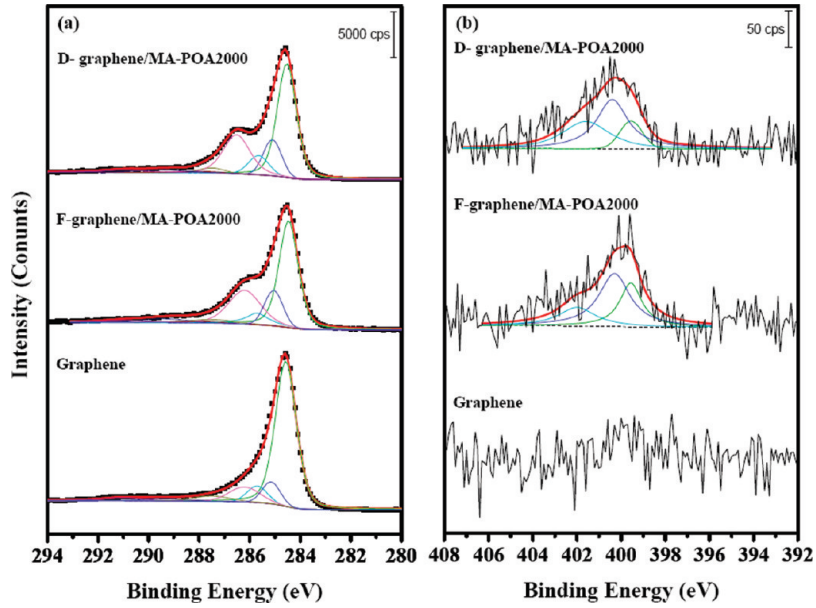

FIGURE 2. High-resolution XPS spectra of the surface of graphene, F-MA-POA2000, and D-MA-POA2000: (a) C1s and (b) N1s.

Table 1. Analysis of the Deconvoluted (a) C1s Peaks and (b) N1s Peaks from XPS and Their Relative Atomic Percentage in Terms of Graphene, F-graphene/MA-POA2000, and D-graphene/MA-POA2000

(a) C1s peaks

	C1s fitting binding energy (eV; relative atomic percentage, %)							
sample name	C═C (sp^2)	C−C (sp^3)	C−O/C−N	C−O−C	C═O	N−C═O	O−C═O	$\pi-\pi^*$
graphene	284.57 (66.8)	285.15 (7.58)	285.7[a] (6.34)	286.2 (8.86)	287.5 (4.34)		289.4 (2.49)	291 (3.54)
F-graphene/MA-POA2000	284.46 (45.6)	285.05 (12.2)	285.7 (7.32)	286.3 (23.5)	287.5 (3.69)	287.9 (1.39)	289.4 (3.62)	291 (2.58)
D-graphene/MA-POA2000	284.53 (47.0)	285.1 (12.3)	285.65 (7.72)	286.52 (22.8)	287.5 (2.39)	287.9 (1.37)	289.4 (3.50)	291 (3.00)

(b) N1s peaks

	N1s fitting binding energy (eV; relative atomic percentage, %)			
sample name	N−C (amine)	N−C═O (amide)	$-NH_x^+$ protonated amine/ hydrogen bonding	$-NH_x^+$/N−C
F-graphene/MA-POA2000	399.56 (29.3)	400.3 (50.0)	402.0 (20.7)	0.706
D-graphene/MA-POA2000	399.55 (13.4)	400.4 (50.0)	401.6 (36.6)	2.73

[a] Only C−O is expected for graphene.

but also, more importantly, they are the restorable sites. Even if the complete picture of the reduction mechanisms involved is still unclear, the mechanisms proposed are nevertheless involved in some way in the reaction between the oxygen-containing functional groups and the reductants (36−39). Therefore, covalent grafting through consumption of these oxygen-containing functional groups in GO implies that these restorable sites are "dead", and the reparation of the sp^2 structures is thus constrained. (iii) Covalent functionalization can be used for graphene prepared by chemical and thermal reduction. To date, very few studies, if any, have addressed a covalently functionalized graphene by using the residual oxygen-containing functional groups as directly reactive sites for the construction of covalent bonding without any pretreatment.

In the study described herein, samples of covalently functionalized graphene were prepared by two different methods using the same molecules. The first method involved typical free radical grafting; the second was the direct reaction of molecules with the residual epoxy groups on graphene. X-ray photoelectron spectroscopy (XPS) and Raman spectroscopy were used to confirm the successful grafting of the molecules on the surface of the graphene. The differences between the morphology and the thermal stability achieved by these two preparation methods were compared using transmission electron microscopy (TEM) and thermogravimetric analysis (TGA).

EXPERIMENTAL SECTION

Materials. Natural graphite powder (Alfa Aesar) was used as the starting material for the preparation of GO. The graphite powder had a particle size of ~70 μm with a purity of 99.99995% and a density of 2.25 g/cm^3. Poly(oxyalkylene)amines (POA) were purchased from the Huntsman Chemical Co., Philadelphia, Pennsylvania, and included poly(oxypropylene) (POP)-backboned diamines with molecular weights, M_w, of 2000 g mol^{-1}. Maleic anhydride (MA) was obtained from Showa Chemical Co., Gyoda City, Saotama, Japan. Anhydrous stabilized tetrahydrofuran (THF) was supplied by Lancaster Co., Eastgare,

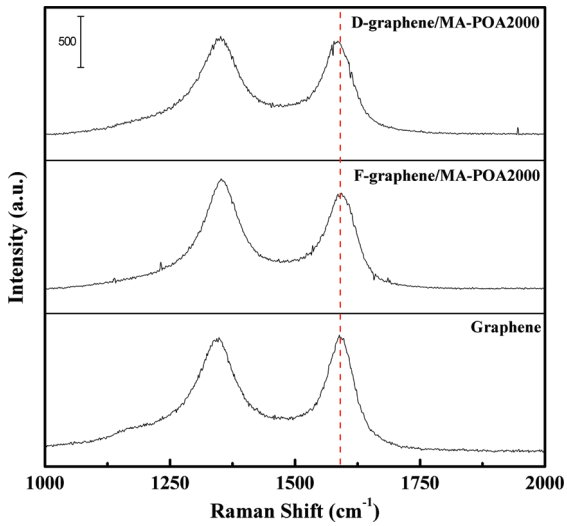

FIGURE 3. Raman spectra of graphene, F-graphene/MA-POA2000, and D-graphene/MA-POA2000.

FIGURE 4. Photograph showing the dispersion of graphene, F-graphene/MA-POA2000, and D-graphene/MA-POA2000 in THF (from right to left). The photograph was taken after storage for 2 monthes with a concentration of 0.25 mg mL^{-1}.

White Lund, Morecambe, England. Benzoyl peroxide (BPO) was obtained from Fluka Chemie. Co., Buchs, Switzerland.

Preparation of Graphite-Oxide (GO) and Thermal Reduction of GO. The natural graphite powder was oxidized using the Staudenmaier method (40) to form GO. Using this method, graphite (5 g) was first mixed with sulfuric acid (87.5 mL) and nitric acid (45 mL) and stirred. When the graphite was dispersed uniformly, potassium chlorate (55 g) was added slowly and stirred for over 96 h. Following completion of the oxidization, the mixture was added into deionized water and then filtered. The GO was rinsed repeatedly and redispersed in a 5% solution of HCl three times. It was then washed continually with deionized water until the pH of the filtrate was neutral. The GO slurry was dried and pulverized. After this process, the GO was dried and pulverized again. Finally, the GO was heated to 1050 °C in an inert gas atmosphere and held in the furnace for 30 s to form graphene.

Preparation of Graphene/MA-POA2000 by Free-Radical Grafting and Direct Modification. The preparation of POA2000 bearing one MA (abbreviated as MA-POA2000) was carried out in a glass reactor equipped with a stirrer. The designated amount of MA (15.68 g, 160 mmol) was slowly added to a reactor charged with POA (160 mmol) and then stirred mechanically at room temperature for 24 h (41).

Scheme 1 depicts an overview of the covalent functional procedure. In order to prepare the free radical graphene/MA-POA2000 (F-graphene/MA-POA2000), 200 mg of graphene was first suspended in 100 mL of THF by shear mixing for 1 h and sonication for 15 min. The free radical reaction was initiated by BPO (1.29 g, 5.34 mmol, twice the amount of MA-POA2000) at 70 °C for 1 h. Subsequently, MA-POA2000 (5.6 g, 2.67 mmol), dissolved in 10 mL of THF, was slowly added to the graphene suspension, and the mixture was further shear mixed at 70 °C by refluxing it for another 8 h.

To prepare the direct reaction graphene/MA-POA2000 (D-graphene/MA-POA2000), another 200 mg of graphene was suspended in 100 mL of THF by shear mixing for 1 h and sonication for 15 min. Subsequently, the excess MA-POA2000 (10 g, 4.77 mmol, estimated from XPS C1s area percentage of epoxy groups (~0.443 mmol) contained in the as-prepared graphene) dissolved in 10 mL of THF was added into the graphene suspension, and the mixture was further shear mixed at 80 °C by refluxing for 24 h.

After each functionalization process was completed, the mixture was separated by filtration through a 0.2 μm polytetrafluoroethylene (PTFE) membrane and thoroughly washed with anhydrous THF several times to remove the residual MA-POA2000 and then dried in a vacuum oven at 80 °C overnight to remove the solvent.

Characterization and Instruments. X-ray diffraction (XRD) was carried out at room temperature at a scan rate of 2° min^{-1} using a Shimadzu XD-5 X-ray diffractometer (40 kV, 30 mA, λ = 0.1542 nm) with a copper target and a Ni filter. X-ray photoelectron spectra (XPS) measurements were performed using a PHI Quantera SXM/AES 650 Auger Electron Spectrometer (ULVAC-PHI Inc., Japan) equipped with a hemispherical electron analyzer and a scanning monochromatic Al Kα (hν = 1486.6 eV) X-ray source. A small spot lens system enabled the analysis of samples that had an area of less than 1 mm^2. The Raman spectra were obtained in a Stellar-PRO confocal Raman microscopy system (MODU-LASER, LLC), and the laser wavelength was 488 nm. Transmission electron microscopy (TEM) analyses were conducted using a JEM-2100 electron microscope at 200 kV, and the samples for the TEM measurements were prepared by one drop casting on a lacey copper grid followed by evaporation of the solvent in the air at room temperature. Thermogravimetric analysis (TGA) was carried out using a DuPont-TGA951 at a heating rate of 10 °C min^{-1} in a N_2 atmosphere.

RESULTS AND DISCUSSION

The degree of exfoliation of GO and the graphene obtained, as well as the funcionalized graphene sheets, were monitored using XRD. As shown in Figure 1a, the graphite exhibited a typical sharp (002) peak at 26.3° with a *d*-spacing of 0.339 nm. As the graphite was converted to GO, the graphite peak shifted downward to 10.0°, with a corresponding *d*-spacing of 0.885 nm, revealing that many of the oxygen atoms were intercalated into the interlayer space and became bound to the graphite planar surface. A shoulder with a small peak was still observed at approximately 20.1°, suggesting that a fraction of the GO was not fully intercalated. Graphene typically shows a broad peak slightly lower than the peak obtained from raw graphite at around 23.9° with a *d*-spacing of 0.372 nm, implying that the graphene was comprised of randomly ordered graphitic platelets in a corrugated structure. The structures of graphene that are shown in Figure 1b and c exhibit a wrinkled surface with a thickness of about 1.82 nm, composed of 4−5 individual

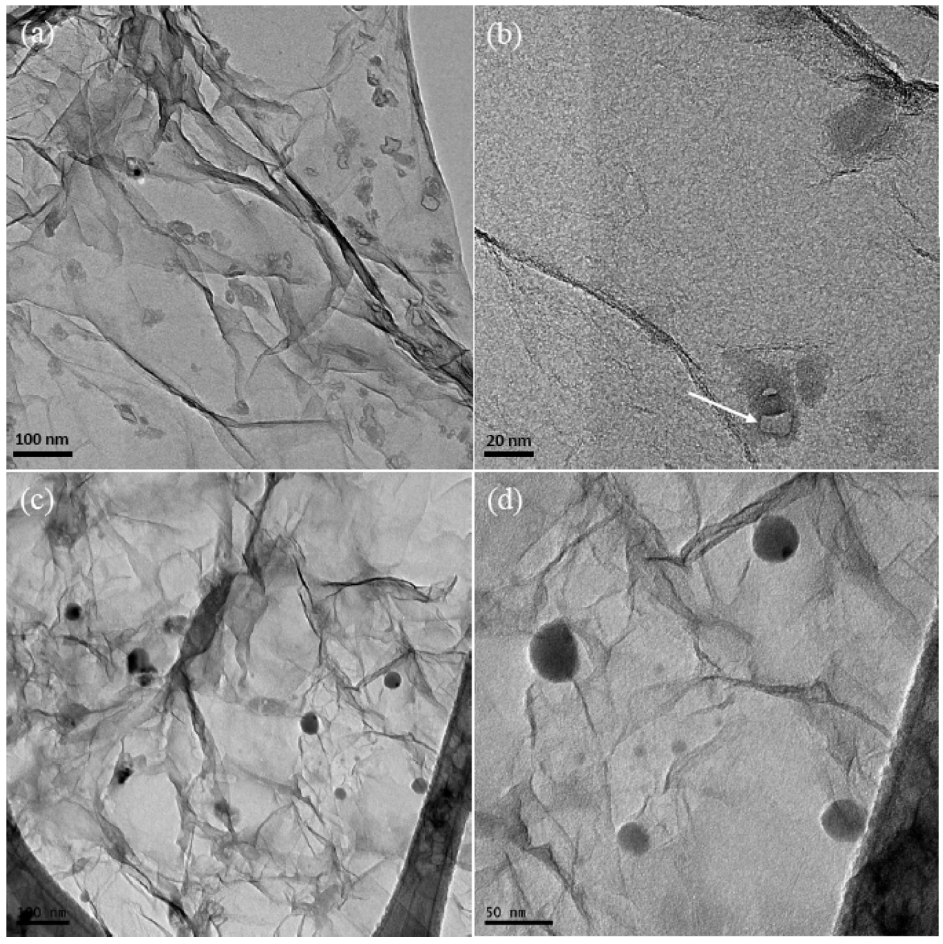

FIGURE 5. TEM images of (a, b) F-graphene/MA-POA2000 and (c, d) D-graphene/MA-POA2000.

graphene sheets. The selected area diffraction pattern (SAED) pattern in Figure 1d also demonstrates that the graphene preserves a crystalline hexagonal structure with Bernal (AB) stacking, as revealed by bright spots in a triangular geometry (42). After functionalization, as depicted in Figure 1d, the (002) peaks of F-graphene/MA-POA2000 and D-graphene/MA-POA2000 were located at ca. 22.1−23.5° and are quite spread out, which indicates that the sheets of functionalized graphene persist in a random order.

Qualitative XPS revealed that the sample surface consisted of graphene functionalized by different methods. Figure 2a shows the C1s core level spectra of graphene, F-graphene/MA-POA2000, and D-graphene/MA-POA2000. Detailed information about the deconvoluted C1 peaks is shown in Table 1a. For graphene, apart from the C═C peak at 284.6 eV, the C−C peak at 285.2 eV, and the $\pi-\pi^*$ satellite peak at 291 eV, four other peaks can be deconvoluted, indicating the presence of other available oxygen-containing functional groups, namely, hydroxyl (C−O at 285.7 eV), epoxy/ether (C−O−C at 286.2 eV), carbonyl (C═O at 287.5 eV), and carboxylate (O−C═O at 289.4 eV). XPS analysis of the F-graphene/MA-POA2000 and D-graphene/MA-POA2000 shows a lower percentage area of the C═C peak. This decrease is due to the covalently attached MA-POA2000 molecules that coat the surface of graphene. After functionalization, F-graphene/MA-POA2000 and D-graphene/MA-POA2000 contain significantly more C−O−C than graphene, revealing an obvious shoulder at this assignment position. This is because each repeating unit of the long backbone MA-POA2000 chains contains an ether group. Noticeably, the increased C−O/C−N peak area and a newly appearing peak at higher energy (287.9 eV) originate from the amine and amide (N−C═O) structures at the ends of MA-POA2000.

The N1s core-level XPS spectra provide further confirmation of the presence of the amine and amide groups of the functionalized graphene. Figure 2b shows two main N1s peaks at approximately 399.6 and 400.3 eV, due to amine and amide nitrogen, respectively, in F-graphene/MA-POA2000 and D-graphene/MA-POA2000 (detailed information on the deconvoluted N1 peaks is shown in Table 1b). The higher binding energy for amide nitrogen is probably due to the existence of resonance structures and therefore bears a partial positive charge (43, 44). Accordingly, the presence of amine and amide groups also accords well with the expected structure of MA-POA2000. Note that F-graphene/MA-POA2000 shows an extra peak at 402 eV due to the protonated amine ($-NH_3^+$) (45), at the terminal position of MA-POA2000. Compared to this completely positively charged nitrogen, the assignment at 401.6 eV (0.4 eV lower) for D-graphene/MA-POA2000 is characterized as a partial positive charge on the secondary amine nitrogen atoms due to the hydrogen bonding interaction between the secondary amine and the hydroxyl group. Because graphene function-

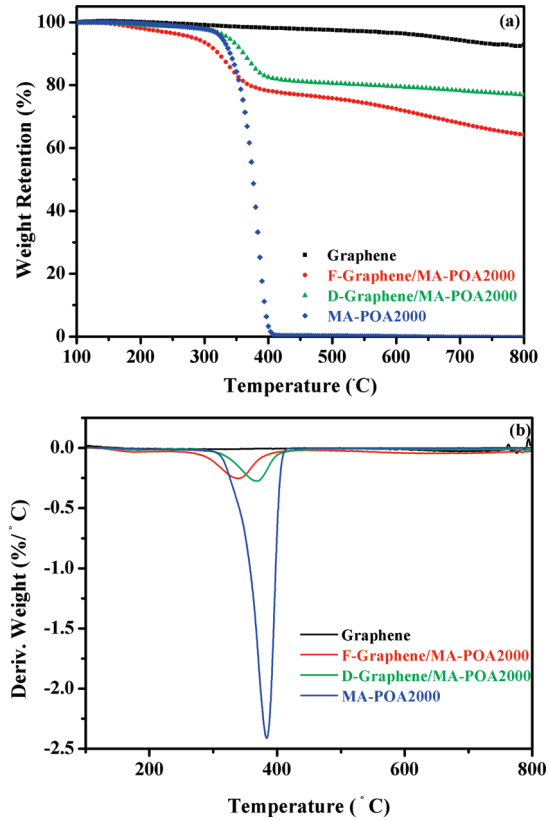

FIGURE 6. (a) Thermogravimetric curves and (b) corresponding derivative curves of graphene, F-Graphene/MA-POA2000, D-Graphene/MA-POA2000, and MA-POA2000.

alization occurs via the direct ring-opening of epoxides, the other side of the secondary amine always bears a hydroxyl group. In addition, it is possible that the lone pair electrons of directly bonded N atoms may resonate with the graphene. Therefore, the secondary amines in D-graphene/MA-POA2000 become charged more easily than the primary amine in F-graphene/MA-POA2000, and this finding may also be characterizated in terms of the $-\underline{N}H_x^+/\underline{N}-C$ area percentage ratio of 2.73 for D-graphene/MA-POA2000 and 0.71 for F-graphene/MA-POA2000.

Raman spectroscopy is a powerful tool for investigating the structural changes that occur in graphene materials because it monitors the D band (~1345 cm^{-1}, breathing mode of A_{1g}) and G band (the in-plane bond-stretching motion of pairs of C sp^2 atoms, E_{2g} mode) (46). By comparing the G-band positions of graphene, F-graphene/MA-POA2000, and D-graphene/MA-POA2000, as shown in Figure 3, it can be seen that the G-band position of D-graphene/MA-POA2000 is softened (i.e., shifted to lower frequencies) by ~5 cm^{-1} in relation to that of graphene (1590 cm^{-1}). This phenomenon may be explained by the fact that the lone pair electrons of directly bonded N atoms resonate with the adjunct benzene structure of graphene and affect its electronic structure. A similar result was also reported for electron-donor molecular functionalized graphene (23). In addition, the D-band of graphene mainly arises from the preparation of graphene that uses a strong oxidization procedure. An increase in the number of defects leads to an increases in the D-band intensity (47). Therefore, F-graphene/MA-POA2000 clearly shows an increase in D-band intensity compared with graphene, indicating that the covalent grafting of MA-POA2000 using a free radical method causes further damage to the graphene surface. This notable increase in D-band intensity has also been described by authors of previous studies, in which graphene was functionalized using covalent grafting on the surface (13, 27, 28) or free radical reactions (48). Quantification of the intensity ratio of the D-band to G-band (*i.e.* I_D/I_G) reveals the extent of the defects in graphene surface modification. The I_D/I_G ratio of graphene is ca. 0.98. For the F-graphene/MA-POA2000 and D-graphene/MA-POA2000, the I_D/I_G ratios are ~1.18 and ~1.02, and the corresponding percentage increases (relative to graphene) are 20.4% and 4.08%, respectively. With free radical grafting, the carbon double bonds on the graphene surface are generally broken to produce covalent reacting sites with the MA-POA2000 molecules. However, the residual epoxy groups on the graphene surface provide reactive sites that bond with amino groups on MA-POA2000. Therefore, it is not necessary to produce additional reactive sites or functional groups on the graphene surface, and there is only a slight increase in the I_D/I_G ratio of D-graphene/MA-POA2000. In contrast, the slightly increased I_D/I_G ratio may be attributed to the formation of covalent bonds (13) between graphene and MA-POA2000 by the direct ring-opening reaction, rather than to any further damage to the structure of the graphene surface. Apparently, the residual epoxy groups on the graphene surface directly provide reactive sites to bond with amino groups on MA-POA2000, and it is thus unnecessary to generate additional reactive sites or functional groups on the surface of the graphene.

Figure 4 shows the dispersion ability in THF for graphene, F-graphene/MA-POA2000, and D-graphene/MA-POA2000 (from right to left). Clearly, deposits of graphene may be seen at the bottom of the solution. This is because the use of residual oxygen-containing functional groups on graphene as suspension media is not sufficient to maintain its long-term stability in an organic solvent. In comparison, F-graphene/MA-POA2000 and D-graphene/MA-POA2000 exhibit a homogeneous dispersion in THF after more than two months. This implies that the long chain of MA-POA2000 effectively improves the compatibility between graphene and THF.

The morphology of graphene and functionalized graphene was characterized using TEM. As shown in Figure 5, the morphologies of F-graphene/MA-POA2000 and D-graphene/MA-POA2000 are rather different from that of graphene (Figure 1b and c), in that covalently attached MA-POA2000 molecules are clearly visible on the graphene surface. Moreover, there are many cavities present on the surface of F-graphene/MA-POA2000 surrounded by MA-POA2000 molecules (shown by the white arrow in Figure 5b). This phenomenon indicates that the functionalization of graphene through a free radical grafting process causes severe damage to the graphene sp^2 structures in generating the reactive sites on the basal plane of the graphene. In contrast, the functionalization of graphene via the residual functional groups

Table 2. Selected Results of TGA Testing

sample	MA-POA2000 decomposition onset (°C)	temp at max wt loss of MA-POA2000 (°C)[a]	wt loss of MA-POA2000 (wt %)[b]	grafting mol %[c]	graphene decomposition onset (°C)	wt loss of graphene[d]
graphene					605	3.69
F-Graphene/MA-POA2000	303	339	17.8	0.102	546	10.3
D-Graphene/MA-POA2000	324	370	17.2	0.098	604	2.64
MA-POA2000	323	384	97.6			

[a] The temperature at the maximum weight loss rate is the temperature at the maximum of the derivative curve. [b] Calculated in the temperature range between 300 and 500 °C. [c] Calculated using the equation, i.e., [MA-POA2000]graphene = [(wt % of MA-POA2000 from TGA/mol wt of MA-POA2000 fragment)/(100/mol wt of carbon)] × 100, which was reported by Baskar et al. (52). [d] Determined by the weight difference between column 6 and the final temperature at 800 °C.

and their direct use as reactive sites can prevent the destruction of the restored sp^2 structures, which can be seen in Figure 5c and d. The surface of D-graphene/MA-POA2000 contains no cavities.

The difference in morphology between F-graphene/MA-POA2000 and D-graphene/MA-POA2000 directly influences their thermal stability. Figure 6 shows the TGA curves and normalized sample mass loss rate divided by the heating rate for graphene, F-graphene/MA-POA2000, D-graphene/MA-POA2000, and MA-POA2000. Table 2 also shows some of the results obtained from TGA testing. For MA-POA2000, the onset of the weight loss is at 323 °C, with the maximum weight loss rate occurring at 384 °C. Graphene exhibits a high thermal stability. The weight loss of 3.47 wt % below 600 °C illustrates the residual oxygen-containing functional groups on graphene. The onset of weight loss occurs at 605 °C relative to the thermal decomposition of graphene, and a 3.69 wt % weight loss was observed up to 800 °C. For the functionalized graphene samples, the slower decomposition rates in the temperature range 300−500 °C indicate that the graphene structure acts as an acceptor of free radicals (49−51) during the oxidative degradation of MA-POA2000 molecules. The weight reductions can be calculated for the grafted MA-POA2000 and were 17.8 wt % for F-graphene/MA-POA2000 and 17.2 wt % for D-graphene/MA-POA2000, and the corresponding mol % of MA-POA2000 molecules with respect to the carbon atoms in graphene were 0.102 mol % and 0.098 mol %, respectively. However, for F-graphene/MA-POA2000, both the onset of decomposition and the temperature at which the maximum rate of weight loss occurred decreased significantly (from 323 to 303 °C and from 384 to 339 °C). More importantly, the onset of weight loss relative to graphene decomposition also dramatically decreased from 605 to 546 °C and was calculated as a 10.3 wt % weight loss at 800 °C. These results demonstrate that the functionalization of graphene by free-radical grafting reduces the thermal stability of MA-POA2000 as well as that of graphene itself. In contrast, for D-graphene/MA-POA2000, not only did the onset of decomposition of MA-POA2000 remain fairly constant but that of the graphene itself did also. The nondestroyed graphene structure preserves its high thermal stability even after covalent functionalization, and the weight loss due to graphene decomposition was only 2.64 wt %. The lower temperature of maximum rate of weight loss (from 384 to 370 °C) may contribute to its increased thermal conductivity due to the presence of graphene. It may therefore be concluded that covalent functionalization via the direct reaction of the residual oxygen-containing functional groups with the chemical molecules provides a greater thermal stability compared to other "grafting" methods, such as the use of free radicals and diazonium etc. Covalent functionalization in this way combines the advantages of noncovalent functionalization (a nondestruct process) and covalent functionalization (a strong interfacial interaction between graphene and the constructed grafted molecules).

CONCLUSIONS

In summary, we have demonstrated a generic approach to address the covalent functionalization of graphene without damaging its structure. The direct use of residual oxygen-containing groups on the graphene surface, e.g., hydroxyl, epoxy, carbonyl, and carboxylate groups, etc., to react with the functional groups on the molecules to be grafted can produce a functionalized graphene with good solvability in, and compatibility with, an organic solvent. Compared to the free-radical grafting method, after direct covalent functionalization, the nondestroyed graphene structure provides greater thermal stability not only for the grafted molecules but also, more importantly, for the graphene itself. The approach described herein could also improve the reinforcement efficiency of graphene in other applications, such as in graphene/polymer composites.

Acknowledgment. The authors are grateful to the National Defense University for the graphene sample supplement.

REFERENCES AND NOTES

(1) Geim, K.; Novoselov, K. S. *Nat. Mater.* **2007**, *6*, 183–191.
(2) Du, X.; Skachko, I.; Barker, A.; Andrei, E. Y. *Nat. Nanotechnol.* **2008**, *3*, 491–495.
(3) Bolotin, K. I.; Sikes, K. J.; Jiang, Z.; Klima, M.; Fudenberg, G.; Hone, J.; Kim, P.; Stormer, H. L. *Solid State Commun.* **2008**, *146*, 351–355.
(4) Balandin, A. A.; Ghosh, S.; Bao, W.; Calizo, I.; Teweldebrhan, D.; Miao, F.; Lau, C. N. *Nano Lett.* **2008**, *8*, 902.
(5) Lee, C.; Wei, X.; Kysar, J. W.; Hone, J. *Science* **2008**, *321*, 385–388.
(6) Stankovich, S.; Dikin, D. A.; Dommett, G H. B.; Kohlhaas, K. M.; Zimney, E. J.; Stach, E. A.; Piner, R D.; Nguyen, S. T.; Ruoff, R. S. *Nature* **2006**, *442*, 282–286.
(7) Novoselov, K. S.; Geim, A. K.; Morozov, S. V.; Jiang, D.; Zhang, Y.; Dubonos, S. V.; Grigorieva, I. V.; Firsov, A. A. *Science* **2004**, *306*, 666–669.
(8) Novoselov, K. S.; Jiang, D.; Schedin, F.; Booth, T. J.; Khotkevich, V. V.; Morozov, S. V.; Geim, A. K. *Proc. Natl. Acad. Sci. U. S. A.* **2005**, *102*, 10451–10453.

(9) Hernandez, Y.; Nicolosi, V.; Lotya, M.; Blighe, F. M.; Sun, Z.; De, S.; McGovern, I. T.; Holland, B.; Byrne, M.; Gun'ko, Y. K.; Boland, J. J.; Niraj, P.; Duesberg, G.; Krishnamurthy, S.; Goodhue, R.; Hutchison, J.; Scardaci, V.; Ferrari, A. C.; Coleman, J. N. *Nat. Nanotechnol.* **2008**, *3*, 563–568.
(10) Bourlinos, A. B.; Georgakilas, V.; Zboril, R.; Steriotis, T. A.; Stubos, A. K. *Small* **2009**, *5*, 1841–1845.
(11) Berger, C.; Song, Z. M.; Li, X. B.; Wu, X. S.; Brown, N.; Naud, C.; Mayou, D.; Li, T. B.; Hass, J.; Marchenkov, A. N.; Conrad, E. H.; First, P. N.; de Heer, W. A. *Science* **2006**, *312*, 1191–1196.
(12) Sutter, P. W.; Flege, J. I.; Sutter, E. A. *Nat. Mater.* **2008**, *7*, 406–411.
(13) Fang, M.; Wang, K.; Lu, H.; Yang, Y.; Nutt, S. *J. Mater. Chem.* **2009**, *19*, 7098–7105.
(14) Bourlinos, A. B.; Gournis, D.; Petridis, D.; Szabo', T.; Szeri, A.; De'ka'ny, I. *Langmuir* **2003**, *19*, 6050–6055.
(15) Wang, G.; Yang, J.; Park, J.; Gou, X.; Wang, B.; Liu, H.; Yao, J. *J. Phys. Chem. C* **2008**, *112*, 8192–8195.
(16) Fan, X.; Peng, W.; Li, Y.; Li, X.; Wang, S.; Zhang, G.; Zhang, F. *Adv. Mater.* **2008**, *20*, 4490–4493.
(17) Rafiee, M. A.; Rafiee, J.; Srivastava, I.; Wang, Z.; Song, H.; Yu, Z. Z.; Koratkar, N. *ACS Nano* **2009**, *3*, 3884–3890.
(18) McAllister, M. J.; Li, J. L.; Adamson, D. H.; Schniepp, H. C.; Abdala, A. A.; Liu, J.; Alonso, M. H.; Milius, D. L.; Car, R.; Prud'homme, R. K.; Aksay, I. A. *Chem. Mater.* **2007**, *19*, 4396–4404.
(19) Rafiee, M. A.; Rafiee, J.; Srivastava, I.; Wang, Z.; Song, H.; Yu, Z. Z.; Koratkar, N. *Small* **2010**, *6*, 179–183.
(20) Ramanathan, T.; Abdala, A. A.; Stankovich, S.; Dikin, D. A.; Herrera-Alonso, M.; Piner, R. D.; Adamson, D. H.; Schniepp, H. C.; Chen, X.; Ruoff, R. S.; Nguyen, S. T.; Aksay, I. A.; PRUD'Homme, R. K.; Brinson, L. C. *Nat. Nanotechnol.* **2008**, *3*, 327–331.
(21) Steurer, P.; Wissert, R.; Thomann, R.; Mü lhaupt, R. *Macromol. Rapid Commun.* **2009**, *30*, 316–327.
(22) Zhao, X.; Zhang, Q.; Chen, D. *Macromolecules* **2010**, *43*, 2357–2363.
(23) Su, Q.; Pang, S.; Alijani, V.; Li, C.; Feng, X.; Mü llen, K. *Adv. Mater.* **2009**, *21*, 3191–3195.
(24) Choi, E. Y.; Han, T. H.; Hong, J.; Kim, J. E.; Lee, S. H.; Kim, H. W.; Kim, S. O. *J. Mater. Chem.* **2010**, *20*, 1907–1912.
(25) Ghosh, A.; Rao, K. V.; George, S. J.; Rao, C. N. R. *Chem.—Eur. J.* **2010**, *16*, 2700–2704.
(26) Yang, Q.; Pan, X.; Huang, F.; Li, K. *J. Phys. Chem. C* **2010**, *114*, 3811–3816.
(27) Sharma, R.; Baik, J. H.; Perera, C. J.; Strano, M. S. *Nano Lett.* **2010**, *10*, 398–405.
(28) Shen, J.; Hu, Y.; Li, C.; Qin, C.; Ye, M. *Small* **2009**, *5*, 82–85.
(29) Loh, K. P.; Bao, Q.; Ang, P. K.; Yang, J. *J. Mater. Chem.* **2010**, *20*, 2277–2289.
(30) Salavagione, H. J.; Gómez, M. A.; Martiñez, G. *Macromolecules* **2009**, *42*, 6331–6334.
(31) Liu, Z. B.; Xu, Y. F.; Zhang, X. Y.; Zhang, X. L.; Chen, Y. S.; Tian, J. G. *J. Phys. Chem. B* **2009**, *113*, 9681–9686.
(32) Dreyer, D. R.; Park, S.; Bielawski, C. W.; Ruoff, R. S. *Chem. Soc. Rev.* **2010**, *39*, 228–240.
(33) Compton, O. C.; Dikin, D. A.; Putz, K. W.; Brinson, L. C.; Nguyen, S. T. *Adv. Mater.* **2010**, *22*, 892–896.
(34) McAllister, M. J.; Li, J. L.; Adamson, D. H.; Schniepp, H. C.; Abdala, A. A.; Liu, J.; Alonso, M. H.; Milius, D. L.; Car, R.; Prud'homme, R. K.; Aksay, I. A. *Chem. Mater.* **2007**, *19*, 4396–4404.
(35) Boukhvalov, D. W.; Katsnelson, M. I. *J. Am. Chem. Soc.* **2008**, *130*, 10697–10701.
(36) Gao, X.; Jang, J.; Nagase, S. *J. Phys. Chem. C* **2010**, *114*, 832–842.
(37) Stankovich, S.; Dikin, D. A.; Piner, R. D.; Kohlhaas, K. A.; Kleinhammes, A.; Jia, Y.; Wu, Y.; Nguyen, S-B. T.; Ruoff, R. S. *Carbon* **2007**, *45*, 1558–1565.
(38) Che, J.; Shen, L.; Xiao, Y. H. *J. Mater. Chem.* **2010**, *20*, 1772–1727.
(39) Gao, J.; Liu, F.; Liu, Y.; Ma, N.; Wang, Z.; Zhang, X. *Chem. Mater.* **2010**, *22*, 2213–2218.
(40) Staudenmaier, L. *Ber. Dtsch. Chem. Ges.* **1898**, *31*, 1481–1487.
(41) Liao, S. H.; Yen, C. Y.; Hung, C. H.; Weng, C. C.; Tsai, M. C.; Lin, Y. F.; Ma, C. C. M.; Pan, C.; Su, A. *J. Mater. Chem.* **2008**, *18*, 3993–4002.
(42) Jeong, H. K.; Lee, Y. P.; Lahaye, R. J. W. E.; Park, M. H.; An, K. H.; Kim, I. J.; Yang, C. W.; Park, C. Y.; Ruoff, R. S.; Lee, Y. H. *J. Am. Chem. Soc.* **2008**, *130*, 1362–1366.
(43) Zhang, X.; Li, H.; Zhao, B.; Shen, J.; Gao, Z.; Li, X. *Macromolecules* **1997**, *30*, 1633–1636.
(44) Liu, Y.; Goh, S. H.; Lee, S. Y. *Macromolecules* **1999**, *32*, 1967–1971.
(45) Zhang, F.; Srinivasan, M. P. *Langmuir* **2007**, *23*, 10102–10108.
(46) Ferrari, A. C.; Robertson, J. *Phys. Rev. B* **2000**, *61*, 14095–14107.
(47) Su, C. Y.; Xu, Y.; Zhang, W.; Zhao, J.; Tang, X.; Tsai, C. H.; Li, L. J. *Chem. Mater.* **2009**, *21*, 5674–5680.
(48) Liu, H.; Ryu, S.; Chen, Z.; Steigerwald, M. L.; Nuckolls, C.; Brus, L. E. *J. Am. Chem. Soc.* **2009**, *131*, 17099–17101.
(49) Jiang, D.; Sumpter, B. G.; Dai, S. *J. Phys. Chem. B* **2006**, *110*, 23628–23632.
(50) Denis, P. A. *J. Phys. Chem. C* **2009**, *113*, 5612–5619.
(51) Galano, A. *Nanoscale* **2010**, *2*, 373–380.
(52) Baskar, D.; Mays, J. W.; Bratcher, M. S. *Angew. Chem., Int. Ed.* **2004**, *43*, 2138–2142.

AM100597D